Inorganic Chemistry

pubs.acs.org/IC

Forum Article

Generation of H_2S from Thiol-Dependent NO Reactivity of Model [4Fe-4S] Cluster and Roussin's Black Anion

Kady M. Oakley, Ziyi Zhao, Ryan L. Lehane, Ji Ma, and Eunsuk Kim*

Cite This: https://doi.org/10.1021/acs.inorgchem.1c01328

Read Online

ACCESS | Metrics & More | Article Recommendations | Supporting Information

ABSTRACT: Iron−sulfur clusters (Fe−S) have been well established as a target for nitric oxide (NO) in biological systems. Complementary to protein-bound studies, synthetic models have provided a platform to study what iron nitrosylated products and byproducts are produced depending on a controlled reaction environment. We have previously shown a model [2Fe-2S] system that produced a dinitrosyl iron complex (DNIC) upon nitrosylation along with hydrogen sulfide (H_2S), another important gasotransmitter, in the presence of thiol, and hypothesized a similar reactivity pattern with [4Fe-4S] clusters which have largely produced inconsistent reaction products across biological and synthetic systems. Roussin's black anion (RBA), $[Fe_4(\mu_3\text{-}S)_3(NO)_7]^-$, is a previously established reaction product from synthetic [4Fe-4S] clusters with NO. Here, we present a new reactivity for the nitrosylation of a synthetic [4Fe-4S] cluster in the presence of thiol and thiolate. $[Et_4N]_2[Fe_4S_4(SPh)_4]$ (**1**) was nitrosylated in the presence of excess PhSH to generate H_2S and an "RBA-like" intermediate that when further reacted with $[NEt_4][SPh]$ produced a $\{Fe(NO)_2\}^9$ DNIC, $[Et_4N][Fe(NO)_2(SPh)_2]$ (**2**). This "RBA-like" intermediate proved difficult to isolate but shares striking similarities to RBA in the presence of thiol based on IR $\upsilon_{(NO)}$ stretching frequencies. Surprisingly, the same reaction products were produced when the reaction started with RBA and thiol. Similar to **1**/NO, RBA in the presence of thiol and thiolate generates stoichiometric amounts of DNIC while releasing its bridging sulfides as H_2S. These results suggest not only that RBA may not be the final product of [4Fe-4S] + NO but also that RBA has unprecedented reactivity with thiols and thiolates which may explain current challenges around identifying biological nitrosylated Fe−S clusters.

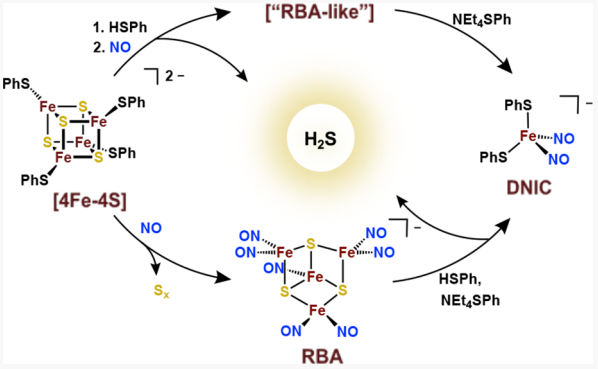

INTRODUCTION

Nitric oxide (NO), originally thought to simply be a toxic gas,[1] has been actively investigated for its role in cellular signaling in the past several decades.[2] Along with carbon monoxide (CO) and hydrogen sulfide (H_2S), NO has been labeled as one of the three important gasotrasmitters in biological systems. Specifically, NO is known to be most active in the central nervous system, where it effects brain development, memory, and learning;[3] in immune response, where it plays a part in the inflammatory response;[4] and in the circulatory system, where it acts as a vasorelaxer and vasodilater to aid circulation.[5] Currently known mechanisms of H_2S production stem from both enzymatic and nonenzymatic pathways. At least three enzymes, cystathionine β-synthase (CBS), cystathione γ-lyase (CSE), and 3-mercaptopyruvate sulfurtransferase (MST), are involved in the biosynthesis of H_2S from L-cysteine (CBS and CSE) or 3-mercaptopyruvate (MST).[6] H_2S can be stored as sulfane sulfur via oxidative post-translation modification of cysteines to form persulfies that can release H_2S under reducing conditions.[6] Interestingly, many of the biological functions performed by H_2S overlap with the functions of NO.[7] Due to this overlap, researchers have been looking for a point of crosstalk for the two for years.[8]

Mechanisms for the NO-H_2S crosstalk can be divided into two categories. One is the crosstalk through protein regulations as seen with the action of NO and H_2S on the secondary messenger cGMP.[9] In this case, NO facilitates the production of cGMP by activating soluble guanylyl cyclase. Once cGMP has been produced, H_2S acts to delay cGMP's degradation by inhibiting phosphodiesterase.[10] The other type of crosstalk is a direct chemical interaction between H_2S and NO and its metabolites. Research into the possibility of this type of crosstalk includes the reactivity of H_2S with NO,[11] nitroprusside,[12] S-nitrosothiols,[13] and peroxynitrite.[14] Our research group has focused on a different possible target for NO-H_2S crosstalk: iron sulfur clusters.

Iron sulfur ([Fe−S]) clusters are ubiquitous in biological systems. Common to the most ancient and modern forms of

Special Issue: Renaissance in NO Chemistry

Received: May 2, 2021

life, they carry out many functions required for survival: electron transport, substrate activation and catalysis, and cellular sensing and signaling.[15] Among the functions of [Fe−S] clusters in biological systems, they have been found to be a major target for reactivity of nitric oxide to form various iron nitrosyl species (Chart 1). The conversion of [Fe−S]

Chart 1. Most Common Forms of Iron Nitrosyls

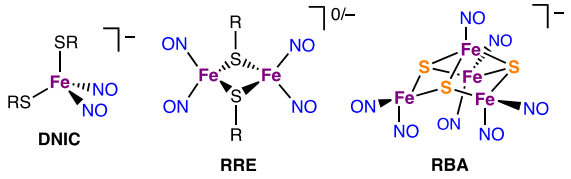

cluster to iron-nitrosyls results in significant changes in protein function that can lead to NO-derived physiological signal transduction[16] or severe toxicity.[17] To study the reactivity of [Fe−S] clusters with NO, researchers have broadly taken two different routes: protein bound clusters to study reactivity in their native environment, and synthetic model clusters to allow the chemical reactivity and mechanisms to be more easily studied. Synthetic models are rarely stable or soluble in biologically relevant aqueous or buffer systems and cannot emulate the structural constrains imposed by the large protein backbones. However, discrete synthetic models that are not being masked by the bulky protein residues and buffer molecules make it possible to study chemical reactivities intrinsic to the [Fe−S] cofactors. These model systems are especially valuable when the reactions involve small gaseous molecules such as O_2, NO, H_2S, etc.

In the past decade, our laboratory used this synthetic modeling approach to provide chemical insights into how cellular redox components such as [Fe−S] clusters, NO, O_2, and H_2S propagate their redox signals.[18] One of the conceptual advances we made was the identification of new reaction conditions that lead to the formation of previously unrecognized products during the reaction of [Fe−S] clusters with NO.[18,19] We found that the bridging sulfides from [2Fe-2S] clusters can be released as H_2S upon nitrosylation if the environment can provide a formal equivalent of H• (e^-/H^+) from donors such as thiols or phenols.[18,19b] These results led us to hypothesize that [Fe−S] clusters can act as a point of direct crosstalk between NO and H_2S. In this Forum article, we report our recent studies probing whether this reactivity can be expanded to other clusters including the cubane-type [4Fe-4S] cluster: the most common cluster form.

RESULTS AND DISCUSSION

Effects of Thiol Inclusion on NO reactivity of [4Fe-4S] Cluster. The first question we sought to answer was whether or not adding an external thiol source to the reaction of [4Fe-4S] cluster with NO would change the reactivity pattern as was observed with [2Fe-2S] clusters.[19b] To make that determination, nitric oxide was added to a synthetic [4Fe-4S] cluster, $[Et_4N]_2[Fe_4S_4(SPh)_4]$ (**1**), in the presence and the absence of an external thiol, PhSH. Both a purified NO gas and a chemical NO donor, S-trityl thionitrite (Ph_3CSNO),[20] were utilized to examine the thiol effects. It is noted that $NO_{(g)}$ and Ph_3CSNO resulted in no difference in the reactivity studies reported in this study. Exposure of excess (10 equiv) NO to an acetonitrile solution of **1** in the absence of PhSH yielded Roussin's black anion (RBA) consistent with the previous report by the Lippard group (Scheme 1a).[20] The crude product generated

Scheme 1

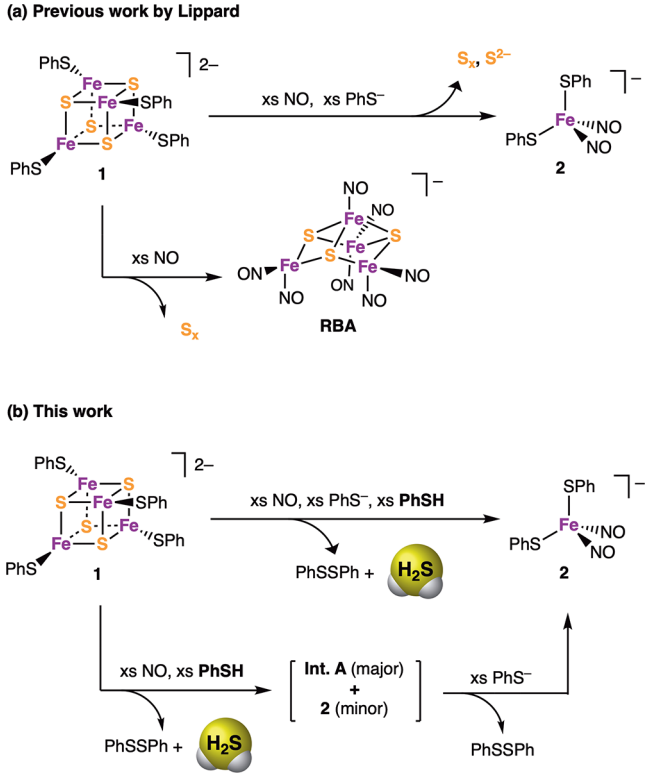

from the reaction of **1** with NO in the presence of thiol (10 equiv) displayed a very similar IR spectrum to that of RBA with ν(NO) stretching frequencies of 1799, 1739, and 1708 cm^{-1} that are slightly shifted lower in energy from RBA (Figure 1A). However, this "RBA-like" product, labeled **Int. A** (Scheme 1b), appears to have drastically different stability from RBA as it constantly changes in morphology and color along with its IR spectrum every recrystallization attempt, hampering us from isolating a purified product. The X-band EPR spectrum of the crude product showed that the major reaction product was EPR silent (at 77 K or RT) while a dinitrosyl iron complex (DNIC), $[Et_4N][Fe(NO)_2(SPh)_2]$ (**2**), was formed as a minor product (~31%); Scheme 1b. DNIC ν(NO) stretching frequencies of 1743 and 1681 cm^{-1} were also observed in the IR spectrum, with the former being encompassed in the broad feature at 1739 cm^{-1} (Figures 1A and S8). Additionally, the fingerprint region of the DNIC thiolate ligands between 1573 and 1388 cm^{-1} is present.

We next investigated the fate of the bridging sulfides in **1** upon nitrosylation in the presence and absence of an external thiol. After the reactions were complete, insoluble material was separated by filtration and subsequently combined with triphenylphosphine, PPh_3, to trap and quantify elemental sulfur that might have been generated from the reaction. ^{31}P NMR spectroscopy and GC-MS were used to determine the formation of triphenylphosphine sulfide, $S{=}PPh_3$, an established reaction product of PPh_3 with elemental sulfur.[19] The **1**/NO reaction in the absence of thiol was found to produce one equivalent of $S{=}PPh_3$ as expected.[20] The **1**/NO reaction in the presence of thiol, however, was found to produce no $S{=}PPh_3$,

https://doi.org/10.1021/acs.inorgchem.1c01328
Inorg. Chem. XXXX, XXX, XXX−XXX

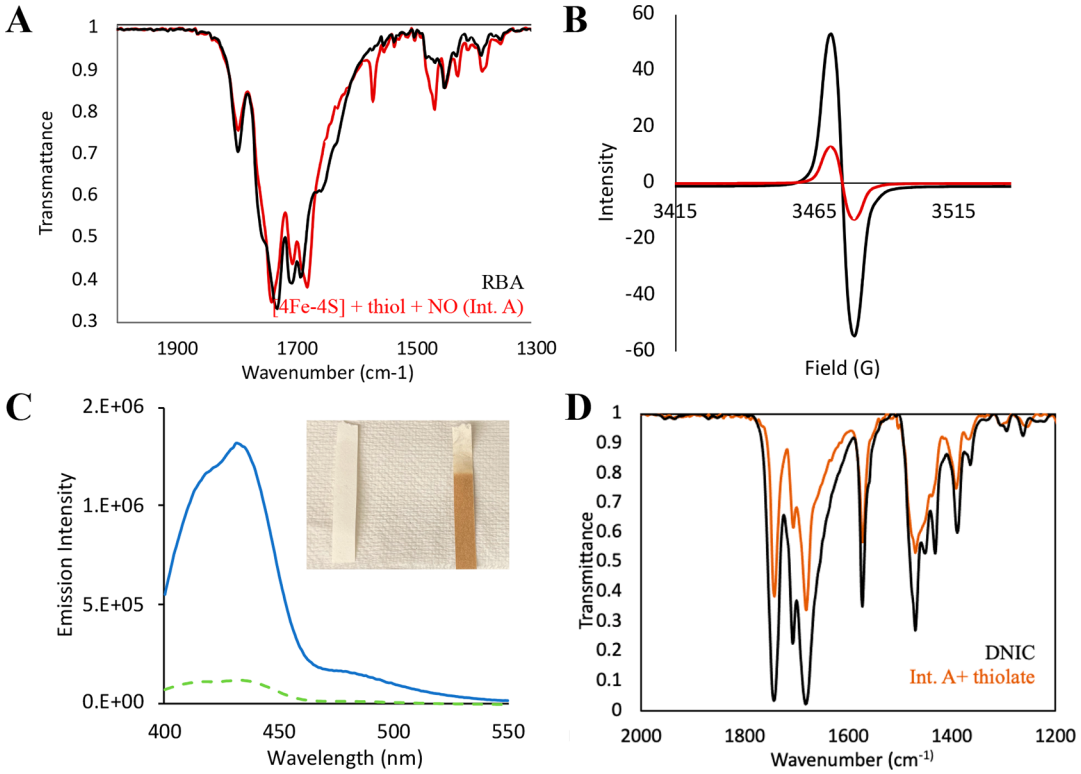

Figure 1. Reaction of $(Et_4N)_2[Fe_4S_4(SPh)_4]$ (**1**) with NO in the presence of thiol and/or thiolate. (A) IR spectrum (in KBr) of **Int. A** (red) resulting from **1**/NO in the presence of HSPh and that of authentic RBA (back). (B) EPR spectra of **1** + 10 equiv PhSH + 10 equiv Ph_3CSNO (red) followed by addition of 10 equiv PhS^- (black) at 298 K. (C) Fluorescence spectra of a turn-on H_2S sensor following incubation with the headspace gas of the **1**/NO reaction in the absence (green) and presence (blue) of HSPh. Inset: Response of lead acetate paper detecting H_2S from **1**/NO in the absence (left) and presence (right) of HSPh. (D) IR spectrum (in KBr) of **Int. A** + 10 equiv PhS^- to generate $[Et_4N][Fe(NO)_2(SPh)_2]$ (**2**) (red) and that of authentic **2** (black).

indicating no elemental sulfur was produced during the reaction.

The negative S_x detection from **1**/NO in the presence of thiol led us to examine H_2S evolution from the thiol containing reaction. We first used lead acetate paper to qualitatively detect H_2S since the interaction of lead acetate with H_2S even in trace concentrations (as low as 5 ppm)[21] can produce dark-brown lead sulfide ($H_2S + Pb(OAc)_2 \rightarrow PbS + 2\ AcOH$). The lead acetate paper strip was hung over the headspace of the reaction flask for the **1**/NO reactions in the absence and presence of excess (10 equiv) PhSH. No color change on the lead acetate paper was observed from **1**/NO in the absence of an external thiol source. However, there was a clear reaction with the lead acetate paper from the **1**/NO reaction with thiol (Figure 1C), indicating that H_2S was produced during the nitrosylation of **1** with PhSH present. Emboldened by this result, we next quantified the amount of H_2S by employing a turn-on H_2S fluorescence sensor, 7-azido-4-methylcoumarin (C7Az).[22] The conversion of the azido group of C7Az to an amino group by H_2S has been reported to enhance a fluorescent emission signal at λ = 434 nm.[22] The headspace gas of the **1**/NO reaction in the presence and absence of thiol was transferred to an acetonitrile solution of C7Az whose fluorescence spectrum was then subsequently analyzed. The **1**/NO reaction in the absence of thiol did not induce any fluorescence signal. However, the same reaction in the presence of thiol led to a significant fluorescence enhancement at 434 nm (Figure 1C). The C7Az sensor exhibited a linear response to increasing concentration of H_2S from 0.2 mM to 1 mM in our experimental setup, which allowed us to quantify the amount of H_2S produced during the course of a reaction using an independently prepared calibration curve using NaSH/HCl. Interestingly, the H_2S quantification revealed that all four equivalents of bridging sulfides in **1** are released as H_2S upon nitrosylation with thiol present, which indicates **Int. A** has no bridging sulfide in its structure.

Effects of Thiolate Inclusion on NO reactivity of [4Fe-4S] Cluster. In spite of the intriguing reactivity of **1**/NO with external thiol leading to H_2S evolution, unidentified **Int. A** has been a considerable challenge for us to gain further insights. Therefore, we turned our attention to convert **Int. A** to another product that is more stable for isolation and characterization. We found that an addition of excess (10 equiv) thiolate, [Et_4N][SPh], to **Int. A** resulted in the formation of a $\{Fe(NO)_2\}^9$ DNIC, $[Et_4N][Fe(NO)_2(SPh)_2]$ (**2**) (Figure 1D). After multiple recrystallizations from MeCN/Et_2O, **2** was isolated (72% yield) as a dark red microcrystalline solid with known spectroscopic characteristics.[23] Complex **2** is one of the most intensively studied DNICs in the literature,[20,23,24] and we capitalized on its unique g = 2.03 EPR signal to quantify the formation of **2** in each step (Scheme 1b) by employing a calibration curve prepared from independently synthesized **2**. Double integration of the g = 2.03 signal from the reaction mixture indicates that ~31% of iron in $[Et_4N]_2[Fe_4S_4(SPh)_4]$ (**1**) is converted to **2** after nitrosylation in the presence of thiol. Upon subsequent treatment with thiolate, there was a significant increase in the g = 2.03 signal which corresponds to the formation of

https://doi.org/10.1021/acs.inorgchem.1c01328
Inorg. Chem. XXXX, XXX, XXX−XXX

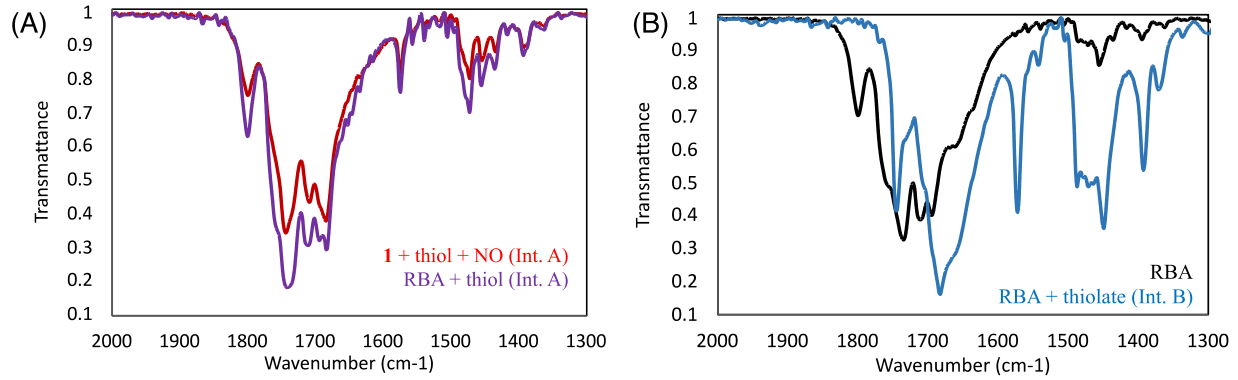

Figure 2. Reaction of RBA with thiol or thiolate. (A) IR spectra (KBr pellet) of the υ_{NO} (cm^{-1}) region comparing RBA + 10 equiv PhSH (purple) to $[Fe_4S_4(SPh)_4]^{2-}$ (**1**) + 10 equiv PhSH + 10 equiv Ph_3CSNO (red). (B) IR spectra comparing RBA + 10 equiv PhS^- (blue) to authentic RBA (black).

overall four equivalents of **2**. The conversion of **1** to **2** can also be achieved in one step when **1** is exposed to NO in the presence of *both* thiol and thiolate. Likewise, the evolution of four equivalents of H_2S was observed from a single step reaction of **1** with NO in the presence of *both* thiol and thiolate. In order to produce the quantitative amounts of **2** and H_2S from **1**, iron must receive electrons from the environment, i.e., externally added thiol/thiolate, which led us to examine the formation of the byproduct, PhSSPh. The GC-MS quantification confirmed the quantitative amount (3 equiv) of disulfide was also produced.[25]

Reaction of Roussin's Black Anion with thiol/thiolate. Roussin's black anion (RBA), $[Fe_4(\mu_3\text{-}S)_3(NO)_7]^-$, is one of the longest known iron nitrosyl compounds[26] and it often appears as a thermodynamic product from NO reactivity with synthetic [Fe−S] clusters.[20] Intrigued by the resemblance of the IR spectrum of RBA to that of **Int. A** (Figure 1A), we decided to investigate the reactivity of RBA with thiol and thiolate to gain further insights into **Int. A**. RBA was prepared by following a literature procedure.[20] To our surprise, when RBA was exposed to free PhSH (10 equiv), the evolution of H_2S was first noticed by the color change of the lead acetate paper. The RBA/HSPh reaction also produces a metastable iron nitrosyl product whose IR spectrum is remarkably similar to that of **Int. A** from the reaction between $[Et_4N]_2[Fe_4S_4(SPh)_4]$ (**1**) and NO in the presence of thiol (Figure 2A). The observed similar stability and the IR features between the two reaction products made us suspect that both reactions might produce the same product. Therefore, we tested whether an addition of thiolate to the product from the reaction of RBA and PhSH would also produce a DNIC, $[Et_4N][Fe(NO)_2(SPh)_2]$ (**2**), as was observed with the reaction of **1**/NO/thiol. Indeed, an addition of excess (20 equiv) [Et4N][SPh] to the reaction product of RBA and PhSH produced **2** without generating any other iron nitrosyl byproduct.

The formation of $[Et_4N][Fe(NO)_2(SPh)_2]$ (**2**) from RBA was not sensitive to the order in which thiol and thiolate were added. The successive addition of the reverse order, i.e., addition of [Et4N][SPh] followed by HSPh or the addition of a mixture of thiol and thiolate to RBA led to the same result: the formation of **2**. When thiolate was added to RBA before thiol addition, however, a new reaction intermediate, **Int. B**, was observed by IR spectroscopy with lower ν(NO) stretching frequencies starting at 1743 cm^{-1} compared to those of RBA that begin at 1799 cm^{-1} (Figure 2B). Previous molecular modeling and semiempirical quantum chemical calculations suggest that a reaction of RBA with thiolate would form a pseudocubane complex, $[Fe_4(\mu_3\text{-}S)_3(\mu_3\text{-}SPh)(NO)_7]^{2-}$ (Chart 2), in which the NO ligands in the thiolate adduct are more

Chart 2

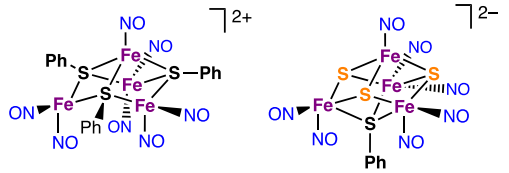

negative than in the RBA cluster.[27] Although we were not able to further characterize Int.B due to its limited stability, our observed ν(NO) stretching frequencies of Int.B suggest more reduced NO characters compared to those in RBA. Accordingly, $[Fe_4(\mu_3\text{-}S)_3(\mu_3\text{-}SPh)(NO)_7]^{2-}$ is considered as a possible structure for **Int.B.** The EPR quantification revealed that 3 equiv of iron embedded in RBA, $[Fe_4(\mu_3\text{-}S)_3(NO)_7]^-$, are eventually converted to $[Et_4N][Fe(NO)_2(SPh)_2]$ (**2**) by the addition of thiol and thiolate. One equivalent of NO is presumed to be released as $NO_{(g)}$, while the remaining one equiv of iron from RBA is released as $[Fe(SPh)_4]^{2-}$, the presence of which was shown in the ^1H NMR spectrum of the crude product mixture (Figure S7). When extra NO is provided to the reaction of RBA with thiol and thiolate, all four equivalents of iron from RBA are converted to **2** as determined by EPR quantification (Scheme 2).

The observed reactivity of RBA, $[Fe_4(\mu_3\text{-}S)_3(NO)_7]^-$, displays how nitrosylation can change the chemical properties of the bridging sulfides in [Fe−S] clusters. The [4Fe-4S] model cluster $[Et_4N]_2[Fe_4S_4(SPh)_4]$ (**1**) is very stable in the presence of large excess PhSH, and the bridging sulfides are not prone to substitution with PhSH. However, the bridging sulfides of RBA are easily released as H_2S by PhSH at room temperature without need for any other reagent. We suspect that the bridging sulfides in RBA are more basic than those in **1** because they are coordinated to iron in a more reduced state (3x $\{Fe(NO)_2\}^9$ and $\{Fe(NO)\}^7$ in RBA) than iron (2+/3+) of compound **1**. This difference might initiate protonation of RBA by a weak acid PhSH ($pK_a \sim 6.6$) to form bridging hydrosulfide, $[Fe_4(\mu_3\text{-}SH)_3(NO)_7]^{2+}$, which could be subsequently replaced by thiolate to form $[Fe_4(\mu_3\text{-}SPh)_3(NO)_7]^{2+}$,

https://doi.org/10.1021/acs.inorgchem.1c01328
Inorg. Chem. XXXX, XXX, XXX−XXX

Scheme 2

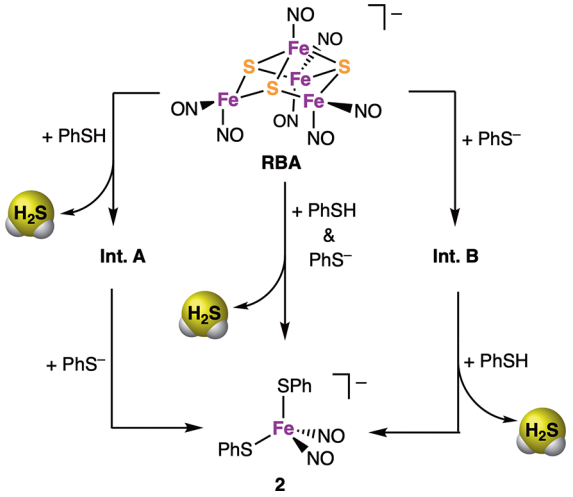

the model we currently consider a possible structure for **Int. A** (Chart 2). The previous study by Lippard established that RBA is the reaction product of **1**/NO.[20] Our study here suggests that RBA may not be the final product and it could be a reactive intermediate leading to other sulfur and iron-containing final products in a thiol rich environment. This unexpected chemical reactivity of RBA may explain the challenges the biochemical and biophysical communities face in identifying products generated from [4Fe-4S] proteins with NO (*vide infra*).

Biological Implications. In spite of a considerable number of studies that report NO reactivity of various [Fe−S] proteins, little is known about the fate of the bridging sulfides after the reaction. Bridging sulfides in [Fe−S] clusters are generally acid-labile, and a strong acid can disrupt the cluster with a release of H_2S. Our study shows that the H_2S evolution from [Fe−S] clusters does not necessarily require a strong acid when [Fe−S] clusters are exposed to NO. Consistent with our previous studies with [2Fe-2S] clusters, we observe that the presence of thiol alters the fate of the bridging sulfides of [4Fe-4S] clusters upon nitrosylation and leads to the H_2S evolution. Given the high concentration of cellular thiols (1−10 mM),[28] our study suggest that H_2S must be a viable reaction product when [Fe−S] cofactors are exposed to NO.

Our reactivity studies of RBA with thiol and/or thiolate originated from a motivation to understand the **1**/NO reactivity with thiol present because RBA was the reaction product from **1**/NO in the absence of thiol.[20] The H_2S evolution from RBA by PhSH came as a surprise. However, this unexpected H_2S formation from RBA has its own intellectual merit considering that RBA has long been known for its antimicrobial activity.[29] The observed H_2S liberation from RBA by thiol suggests that the known antimicrobial effect of RBA might be directly linked to the H_2S redox signaling.[6a,9,30]

The conversion of [Fe−S] clusters to iron-nitrosyl species by NO has drawn considerable attention for the past decade. As for the [2Fe-2S] clusters, there is a clear pattern in NO reactivity. The final nitrosylated products are either $\{Fe(NO)_2\}^9$ DNIC or its dimeric form, species known as Roussin's red ester (RRE), Chart 1, in most cases[16c,31] with the exception of the [2Fe-2S] clusters in mitoNEET and miner2 that reversibly bind NO.[32] Unlike [2Fe-2S] systems, however, nitrosylated products from [4Fe-4S] clusters show no consistency. Nuclear resonance vibrational (NRV) spectroscopic studies on [4Fe-4S]-ferredoxin report RBA as the main nitrosylated product.[33] Another [4Fe-4S] protein, EndoIII, reports a 1:1 mixture of RRE and DNIC as the final nitrosylated products analyzed by HYSCORE pulse EPR spectroscopy and mass spectrometry.[34] As for WhiD and NsrR regulatory proteins, which are dedicated NO-sensors in microorganisms, Mössbauer, NRVS, and DFT, and $^{14}NO/^{15}NO$ and $^{32}S/^{34}S$ labeling studies rule out the formation of RBA from these proteins.[35] Instead, researchers report the nitrosylated products of WhiD and NsrR (both from *S. coelicolor*) as "species related to RBA and RRE".[35] Similarly, another ambiguous "RBA-like" description is given to the nitrosylated product from a [4Fe-4S] HiPIP protein with NO.[36] We conjecture that the various types of unidentified nitrosylated products observed with [4Fe-4S] proteins might be due to the intrinsic instability of multinuclear [Fe−S] clusters with NO ligands. The current study shows that the bridging sulfides embedded in RBA are more reactive toward thiol compared to the bridging sulfides in [Fe−S] clusters without NO ligands. It also shows that the "RBA-like" intermediates can easily convert to another type of iron nitrosyl by thiolate. This structural vulnerability of iron nitrosyls resulting from [4Fe-4S]/NO against environmental factors (thiol, thiolate, etc.) might be a reason for the lack of a general product type.

CONCLUSIONS

Our previous studies demonstrated that both of the bridging sulfides in prototypical [2Fe-2S] clusters such as $[Fe_2S_2(SPh)_4]^{2-}$ can be released as H_2S upon NO exposure if the environment is capable of providing a formal equivalent of H• (e^-/H^+) from donors such as thiols and phenols.[18,19] The present study shows that the formation of H_2S from NO/[Fe−S] reactivity in the presence of thiol is relevant beyond the [2Fe-2S] subclass to now include the [4Fe-4S] type, the most common form of [Fe−S] cluster. Upon nitrosylation of $[Fe_4S_4(SPh)_4]^{2-}$ (**1**) in the presence of PhSH, all four equivalents of the bridging sulfides are released as H_2S with the concomitant formation of a new EPR-silent iron nitrosyl intermediate whose IR features resemble those of RBA. This "RBA-like" intermediate is subsequently converted to a $\{Fe(NO)_2\}^9$ DNIC, $[Fe_2(NO)_2(SPh)_2]^{2-}$ (**2**), upon thiolate addition. The exposure of RBA to PhSH generates H_2S and the same "RBA-like" intermediate. The latter transforms to **2** with further treatment with thiolate. The NO binding to [Fe−S] clusters appears to greatly alter the chemical properties of the bridging sulfides which can be released as H_2S in the presence of thiol.

EXPERIMENTAL SECTION

General. All synthesized products were assumed to be air- and moisture-sensitive. They were manipulated under argon on a standard Schlenk line or in an atmosphere of purified nitrogen in an MBraun Labmaster SP glovebox (O_2 < 1 ppm; H_2O < 1 ppm). Solvents were purified by being passed through a series of two activated alumina columns (MBraun solvent purification system) under an Ar atmosphere and stored over 4 Å molecular sieves. Phenyl disulfide (PhSSPh), thiophenol (HSPh), triphenylphosphine (TPP), triphenylphosphine sulfide (TPPS), sodium hydrosulfide, Celite, 7-azido-4-methylcoumarin (C7Az), and lead acetate paper were purchased from Sigma and used as received. Tube sealant was purchased from Fisher and used as received.

https://doi.org/10.1021/acs.inorgchem.1c01328
Inorg. Chem. XXXX, XXX, XXX−XXX

Physical Measurements. Infrared spectra were recorded on a Bruker Tensor 27 FT-IR spectrometer. Fluorescence spectra were recorded on a Tecan Safire spectrometer. ^{1}H NMR spectra were recorded at 400 MHz on a Bruker UltraShield spectrometer and residual solvent signals were used as an internal reference. EPR spectra of a liquid sample were recorded on a Bruker EMX plus EPR spectrometer at 298 K. The EPR samples were loaded into a 100 μL glass capillary that was inserted into a 4 mm o.d. quartz EPR tube. Spectra were recorded under the following conditions: microwave frequency, 9.871 GHz; microwave power, 2.0 mW; modulation amplitude and frequency, 1.000 G and 100 kHz. GC-MS data were recorded using a Hewlett-Packard (Agilent) GCD 1800C GC-MS spectrometer.

Synthesis. $(Et_4N)_2[Fe_4S_4(SPh)_4]$ (**1**),[37] $(Et_4N)[Fe_4S_3(NO)_7]$ (RBA),[20] $(Et_4N)[Fe(NO)_2(SPh)_2]$ (**2**),[23] and trityl-S-nitrosothiol[20] were prepared as described in the literature.

Reaction of $(Et_4N)_2[Fe_4S_4(SPh)_4]$ (1) with Ph_3CSNO (*a*) in the Absence of Thiol and Thiolate. This reaction has been previously reported by Lippard and co-workers.[20] In the glovebox, a solution of 50 mg (0.045 mmol) of **1** in 5 mL of MeCN was mixed with 102.2 mg (0.243 mmol) of Ph_3CSNO. The reaction was allowed to stir for 3 h at room temperature in dark. During this time, the formation of an insoluble solid (i.e., elemental sulfur) could be observed. This insoluble solid was separated by filtration. The filtrate was saved, and all volatiles were removed *in vacuo*. The resultant residue was washed with Et_2O and redissolved in 1 mL of THF. Crystallization from THF/pentane gave $(Et_4N)[Fe_4S_3(NO)_7]$ (RBA) as black crystals (24.4 mg, 81%); its UV−vis and IR spectroscopic features were in good agreement with those reported for RBA.[20]

Reaction of $(Et_4N)_2[Fe_4S_4(SPh)_4]$ (1) with Ph_3CSNO (*b*) in the Presence of Thiol and Thiolate. Under a N_2 atmosphere, 50 mg (0.045 mmol) of **1** was dissolved in 5 mL of MeCN, and the mixture was transferred to a 25 mL Schlenk flask to which was added 10 equiv of PhSH followed by addition of 10 equiv of Ph_3CSNO and 10 equiv of $[NEt_4][SPh]$. The reaction was stirred at room temperature in the dark for 3 h. During this time, the color of the reaction mixture turned from brown-red to dark red and the formation of H_2S could be qualitatively observed by lead acetate paper (Figure 1A). After 3 h, all volatiles were removed *in vacuo*. The residue was washed with 10 mL of Et_2O and the Et_2O washing was later found to contain the PhSSPh. Analysis of the IR spectrum of the black oily residue indicated $(Et_4N)[Fe(NO)_2(SPh)_2]$ (**2**) to be the only NO-containing product. The oily residue was recrystallized in 5 mL of a 1:1 MeCN:Et_2O solution in a −35 °C freezer overnight to afford **2** as dark red needles (61.2 mg, 72%) whose UV−vis, IR, and EPR spectra were in good agreement with those reported for **2**.[23]

General Method for Product Detection and Quantification for Reaction *b*. Under a N_2 atmosphere, 0.2 mL of a 10 mM $(Et_4N)_2[Fe_4S_4(SPh)_4]$ (**1**) stock solution was mixed with 10 equiv (0.2 mL, 100 mM) of PhSH in a 10 mL Schlenk flask and sealed with a rubber septum, and 10 equiv (0.2 mL, 100 mM) of Ph_3CSNO was injected into the flask. After 3 h of stirring, 1 mL of a $[NEt_4][SPh]$ stock solution (20 mM, 10 equiv) was injected into the reaction mixture. The resulting solution was allowed to further stir for 1 h at room temperature. The reaction products were identified by IR, GS-MS, and EPR spectroscopy.

a. Hydrogen sulfide (H_2S) detection. The formation of H_2S during the reaction could be qualitatively analyzed using lead acetate paper. After the $(Et_4N)_2[Fe_2S_2(SPh)_4]$ (**1**) solution was loaded into the Schlenk flask, a lead acetate paper strip was held in place by a rubber septum in the flask headspace. Addition of Ph_3CSNO, PhSH, and $[NEt_4][SPh]$ were carefully carried out via syringe, while avoiding touching the detector with the reaction solution. The color change of the lead acetate paper was then observed (Figure 1A, inset).

A turn-on fluorescence H_2S sensor, 7-azido-4-methylcoumarin (C7Az),[22] was used to quantify the amount of H_2S produced. In the presence of H_2S, the azide group of C7Az is reduced to an amine and generates 7-amino-4-methylcoumarin (C7Am) that emits at λ_{em} = 434 nm. After reaction completion, a 25 mL two-neck round-bottom flask containing 1 mL of 10 mM C7Az solution in MeCN was connected to the side arm of the reaction flask (Figure S1). The C7Az containing round-bottom flask was placed in liquid nitrogen to generate negative pressure, after which the side arm of the reaction Schlenk flask was opened to allow gas transfer for 2 min. The connection between the C7Az containing round-bottom flask and the reaction Schlenk flask was cut off after gas transfer. The C7Az containing round-bottom flask was removed from liquid nitrogen, and the C7Az solution was allowed to stir for an additional hour at room temperature. The 30-fold diluted C7Az solution in MeCN was used for fluorescence analysis (Figure 1A).

The calibration curve for H_2S detection was made through the same procedure using NaSH and HCl in the reaction flask to produce H_2S for analysis. By varying the amount of NaSH and HCl, H_2S between 0.2 and 1 mM was generated and used for the calibration curve (Figure S2).

The percent yield of H_2S generated during the reaction of [4Fe-4S] cluster with Ph_3CSNO in the presence of thiol and thiolate is approximately 100% based on fluorescence intensity, signifying all 4 bridging-sulfide were released as H_2S. Additionally, we found that all H_2S release was during the first step of the reaction, as in the reaction of [4Fe-4S] cluster with Ph_3CSNO and thiol, while the following addition of $[NEt_4][SPh]$ did not result in any additional H_2S formation.

b. Iron-containing species detection. IR spectrum of the reaction mixture of $(Et_4N)_2[Fe_4S_4(SPh)_4]$ (**1**) reacted with Ph_3CSNO in the presence of thiol showed the generation of a new type of iron-nitrosyl species, Int. A (Figure 1C). The addition of $[NEt_4][SPh]$ produced changes in the IR spectrum that suggest DNIC to be the only iron-containing species after the addition of $[NEt_4][SPh]$ (Figure 1D).

EPR spectroscopy was used to quantify the amount of DNIC, $(Et_4N)[Fe(NO)_2(SPh)_2]$ (**2**), generation (Figure 1B). The calibration curve for **2** (Figure S3) was prepared using independently synthesized **2** dissolved in MeCN in the concentration range of 1−6 mM. In the glovebox, 0.2 mL of 10 mM $(Et_4N)_2[Fe_4S_4(SPh)_4]$ (**1**) stock solution was mixed with 10 equiv (0.2 mL, 100 mM) of PhSH and 10 equiv (0.2 mL, 100 mM) of Ph_3CSNO in a 10 mL Schlenk flask. After stirring in the dark for 3 h, the EPR trace showed a weak EPR signal at g = 2.029 corresponding to ∼31% DNIC production where the formation of 4 equiv of **2** per **1** was considered as 100%. After the first reaction step of [4Fe-4S] with Ph_3CSNO and thiol, 1 mL of $[NEt_4][SPh]$ stock solution (20 mM, 10 equiv) was added into the reaction mixture and allowed to stir for an additional hour. The EPR trace after the addition of $[NEt_4][SPh]$ displayed the same signal at g = 2.029 with stronger intensity, corresponding to 93% DNIC generation for the whole reaction of [4Fe-4S] with Ph_3CSNO in the presence of thiol and thiolate.

c. Phenyldisulfide (PhSSPh) detection. PhSSPh quantification was carried out using GC-MS where the calibration curve for PhSSPh (Figure S4) was made in the concentration range of 50 to 500 μM, while 50 μM of S=PPh_3 was used as an internal standard to provide reproducible data from day-to-day measurements. The calibration curve was based on the normalized peak area of PhSSPh.

After reaction b was finished, a 150 μL aliquot of the reaction solution was mixed with 20 μL of a solution of S=PPh_3 (3.75 mM) in MeCN. The final volume of the mixture was adjusted to 1.5 mL with MeCN to make a GC sample. A control reaction without $(Et_4N)_2[Fe_4S_4(SPh)_4]$ (**1**) was also tested and served as a baseline to detect any PhSSPh formation that resulted from excess HSPh oxidizing under the GC conditions. The amount of PhSSPh generated from the [4Fe-4S] cluster that reacted with Ph_3CSNO in the presence of thiol and thiolate was determined as 91 ± 3%, where 3 equiv of PhSSPh formation per [4Fe-4S] cluster was considered as 100%.

Reaction of $(Et_4N)[Fe_4S_3(NO)_7]$ (RBA) with thiol and thiolate (c) in the presence of Ph_3CSNO. In the glovebox, 0.2 mL of 10 mM RBA stock solution was mixed with 10 equiv (1 mL, 20 mM) of Ph_3CSNO and 20 equiv of $[NEt_4][SPh]$ stock solution (1 mL, 40 mM) in a 10 mL Schlenk flask and sealed with a rubber septum. Ten equiv (0.2 mL, 100 mM) of PhSH was then injected into the flask. The reaction solution was allowed to stir in the dark for 3 h, during which the color of the reaction mixture changed from brown to dark

https://doi.org/10.1021/acs.inorgchem.1c01328
Inorg. Chem. XXXX, XXX, XXX−XXX

red and the formation of H_2S could be observed by lead acetate paper. NMR, IR, and EPR spectra of the reaction mixture confirmed **2** to be the only iron-containing product (Figure S5). EPR quantification suggests a 91 ± 2% of DNIC, $(Et_4N)[Fe(NO)_2(SPh)_2]$ (**2**), formation where 4 equiv of DNIC generation per RBA molecule was considered as 100%.

Reaction of $(Et_4N)[Fe_4S_3(NO)_7]$ (RBA) with thiol and thiolate (d) in the absence of Ph_3CSNO. In the glovebox, 0.2 mL of 10 mM RBA stock solution was mixed with 10 equiv of $[NEt_4][SPh]$ stock solution and 10 equiv (0.2 mL, 100 mM) of PhSH solution. The reaction solution was further diluted with 1 mL of MeCN and stirred in the dark for 3 h. The formation of H_2S could be observed by lead acetate paper during the reaction. NMR spectrum of the reaction showed the formation of $(NEt_4)_2[Fe(SPh)_4]$ (Figure S7), and the iron-nitrosyl product DNIC was confirmed by IR and EPR spectroscopy (Figure S6). EPR quantification suggests 69 ± 2% of DNIC formation where 4 equiv of DNIC generation per RBA molecule was considered as 100%.

■ ASSOCIATED CONTENT

Supporting Information

The Supporting Information is available free of charge at https://pubs.acs.org/doi/10.1021/acs.inorgchem.1c01328.

Calibration curves for H_2S quantification, DNIC quantification, and disulfide quantification. IR and 1H NMR spectra monitoring the reaction of RBA/thiol/thiolate with and without Ph_3CSNO (PDF)

■ AUTHOR INFORMATION

Corresponding Author

Eunsuk Kim − *Department of Chemistry, Brown University, Providence, Rhode Island 02912, United States;* orcid.org/0000-0001-8803-0666; Email: eunsuk_kim@brown.edu

Authors

Kady M. Oakley − *Department of Chemistry, Brown University, Providence, Rhode Island 02912, United States*

Ziyi Zhao − *Department of Chemistry, Brown University, Providence, Rhode Island 02912, United States*

Ryan L. Lehane − *Department of Chemistry, Brown University, Providence, Rhode Island 02912, United States*

Ji Ma − *Department of Chemistry, Brown University, Providence, Rhode Island 02912, United States*

Complete contact information is available at: https://pubs.acs.org/10.1021/acs.inorgchem.1c01328

Funding

The authors thank the NSF (CHE 1807845) for financial support.

Notes

The authors declare no competing financial interest.

■ ACKNOWLEDGMENTS

The authors thank the NSF (CHE 1807845) for financial support.

■ ABBREVIATIONS

cGMP, cyclic guanosine monophosphate; DNIC, dinitrosyl iron complex; RBA, Roussin's black anion; RRE, Roussin's red ester

■ REFERENCES

(1) Culotta, E.; Koshland, D. E., Jr. NO news is good news. *Science* **1992**, *258*, 1862−1865.

(2) Gow, A. J.; Ischiropoulos, H. Nitric oxide chemistry and cellular signaling. *J. Cell. Physiol.* **2001**, *187*, 277−282.

(3) Brenman, J. E.; Bredt, D. S. Nitric oxide signaling in the nervous system. *Methods Enzymol.* **1996**, *269*, 119−129.

(4) MacMicking, J.; Xie, Q. W.; Nathan, C. Nitric oxide and macrophage function. *Annu. Rev. Immunol.* **1997**, *15*, 323−350.

(5) Ignarro, L. J. Biosynthesis and metabolism of endothelium-derived nitric oxide. *Annu. Rev. Pharmacol. Toxicol.* **1990**, *30*, 535−560.

(6) (a) Filipovic, M. R.; Zivanovic, J.; Alvarez, B.; Banerjee, R. Chemical Biology of H2S Signaling through Persulfidation. *Chem. Rev.* **2018**, *118*, 1253−1337. (b) Kimura, H. Hydrogen sulfide: its production, release and functions. *Amino Acids* **2011**, *41*, 113−121.

(7) King, A. L.; Polhemus, D. J.; Bhushan, S.; Otsuka, H.; Kondo, K.; Nicholson, C. K.; Bradley, J. M.; Islam, K. N.; Calvert, J. W.; Tao, Y. X.; Dugas, T. R.; Kelley, E. E.; Elrod, J. W.; Huang, P. L.; Wang, R.; Lefer, D. J. Hydrogen sulfide cytoprotective signaling is endothelial nitric oxide synthase-nitric oxide dependent. *Proc. Natl. Acad. Sci. U. S. A.* **2014**, *111*, 3182−3187.

(8) (a) Kolluru, G. K.; Shen, X.; Kevil, C. G. A tale of two gases: NO and HS, foes or friends for life? *Redox Biol.* **2013**, *1*, 313−318. (b) Pieretti, J. C.; Junho, C. V. C.; Carneiro-Ramos, M. S.; Seabra, A. B. H_2S- and NO-releasing gasotransmitter platform: A crosstalk signaling pathway in the treatment of acute kidney injury. *Pharmacol. Res.* **2020**, *161*, 105121.

(9) Szabo, C. Hydrogen sulphide and its therapeutic potential. *Nat. Rev. Drug Discovery* **2007**, *6*, 917−935.

(10) Coletta, C.; Papapetropoulos, A.; Erdelyi, K.; Olah, G.; Modis, K.; Panopoulos, P.; Asimakopoulou, A.; Gero, D.; Sharina, I.; Martin, E.; Szabo, C. Hydrogen sulfide and nitric oxide are mutually dependent in the regulation of angiogenesis and endothelium-dependent vasorelaxation. *Proc. Natl. Acad. Sci. U. S. A.* **2012**, *109*, 9161−9166.

(11) (a) Yong, Q. C.; Cheong, J. L.; Hua, F.; Deng, L. W.; Khoo, Y. M.; Lee, H. S.; Perry, A.; Wood, M.; Whiteman, M.; Bian, J. S. Regulation of heart function by endogenous gaseous mediators-crosstalk between nitric oxide and hydrogen sulfide. *Antioxid. Redox Signaling* **2011**, *14*, 2081−2091. (b) Yong, Q. C.; Hu, L. F.; Wang, S.; Huang, D.; Bian, J. S. Hydrogen sulfide interacts with nitric oxide in the heart: possible involvement of nitroxyl. *Cardiovasc. Res.* **2010**, *88*, 482−491.

(12) (a) Filipovic, M. R.; Eberhardt, M.; Prokopovic, V.; Mijuskovic, A.; Orescanin-Dusic, Z.; Reeh, P.; Ivanovic-Burmazovic, I. Beyond H_2S and NO interplay: hydrogen sulfide and nitroprusside react directly to give nitroxyl (HNO). A new pharmacological source of HNO. *J. Med. Chem.* **2013**, *56*, 1499−1508. (b) Filipovic, M. R.; Ivanovic-Burmazovic, I. The kinetics and character of the intermediates formed in the reaction between sodium nitroprusside and hydrogen sulfide need further clarification. *Chem. - Eur. J.* **2012**, *18*, 13538−13540.

(13) Filipovic, M. R.; Miljkovic, J.; Nauser, T.; Royzen, M.; Klos, K.; Shubina, T.; Koppenol, W. H.; Lippard, S. J.; Ivanovic-Burmazovic, I. Chemical Characterization of the Smallest S-Nitrosothiol, HSNO; Cellular Cross-talk of H_2S and S-Nitrosothiols. *J. Am. Chem. Soc.* **2012**, *134*, 12016−12027.

(14) (a) Filipovic, M. R.; Miljkovic, J.; Allgauer, A.; Chaurio, R.; Shubina, T.; Herrmann, M.; Ivanovic-Burmazovic, I. Biochemical insight into physiological effects of H_2S: reaction with peroxynitrite and formation of a new nitric oxide donor, sulfinyl nitrite. *Biochem. J.* **2012**, *441*, 609−621. (b) Whiteman, M.; Armstrong, J. S.; Chu, S. H.; Jia-Ling, S.; Wong, B. S.; Cheung, N. S.; Halliwell, B.; Moore, P. K. The novel neuromodulator hydrogen sulfide: an endogenous peroxynitrite 'scavenger'? *J. Neurochem.* **2004**, *90*, 765−768.

(15) Johnson, D. C.; Dean, D. R.; Smith, A. D.; Johnson, M. K. Structure, function, and formation of biological iron-sulfur clusters. *Annu. Rev. Biochem.* **2005**, *74*, 247−281.

(16) (a) Stys, A.; Galy, B.; Starzynski, R. R.; Smuda, E.; Drapier, J. C.; Lipinski, P.; Bouton, C. Iron regulatory protein 1 outcompetes iron regulatory protein 2 in regulating cellular iron homeostasis in response to nitric oxide. *J. Biol. Chem.* **2011**, *286*, 22846−22854. (b) Cruz-Ramos, H.; Crack, J.; Wu, G.; Hughes, M. N.; Scott, C.; Thomson, A. J.; Green, J.; Poole, R. K. NO sensing by FNR: regulation of the Escherichia coli NO-detoxifying flavohaemoglobin, Hmp. *EMBO J.* **2002**, *21*, 3235−3244. (c) Ding, H.; Demple, B. Direct nitric oxide signal transduction via nitrosylation of iron-sulfur centers in the SoxR transcription activator. *Proc. Natl. Acad. Sci. U. S. A.* **2000**, *97*, 5146−5150. (d) Yukl, E. T.; Elbaz, M. A.; Nakano, M. M.; Moenne-Loccoz, P. Transcription Factor NsrR from Bacillus subtilis Senses Nitric Oxide with a 4Fe-4S Cluster. *Biochemistry* **2008**, *47*, 13084−13092. (e) Tucker, N. P.; Hicks, M. G.; Clarke, T. A.; Crack, J. C.; Chandra, G.; Le Brun, N. E.; Dixon, R.; Hutchings, M. I. The transcriptional repressor protein NsrR senses nitric oxide directly via a [2Fe-2S] cluster. *PLoS One* **2008**, *3*, No. e3623. (f) Crack, J. C.; Smith, L. J.; Stapleton, M. R.; Peck, J.; Watmough, N. J.; Buttner, M. J.; Buxton, R. S.; Green, J.; Oganesyan, V. S.; Thomson, A. J.; Le Brun, N. E. Mechanistic insight into the nitrosylation of the [4Fe-4S] cluster of WhiB-like proteins. *J. Am. Chem. Soc.* **2011**, *133*, 1112−1121.

(17) (a) Hyduke, D. R.; Jarboe, L. R.; Tran, L. M.; Chou, K. J.; Liao, J. C. Integrated network analysis identifies nitric oxide response networks and dihydroxyacid dehydratase as a crucial target in Escherichia coli. *Proc. Natl. Acad. Sci. U. S. A.* **2007**, *104*, 8484−8489. (b) Ren, B.; Zhang, N.; Yang, J.; Ding, H. Nitric oxide-induced bacteriostasis and modification of iron-sulphur proteins in Escherichia coli. *Mol. Microbiol.* **2008**, *70*, 953−964. (c) Landry, A. P.; Duan, X.; Huang, H.; Ding, H. Iron-sulfur proteins are the major source of protein-bound dinitrosyl iron complexes formed in Escherichia coli cells under nitric oxide stress. *Free Radical Biol. Med.* **2011**, *50*, 1582−1590. (d) Drapier, J. C.; Hibbs, J. B., Jr. Murine cytotoxic activated macrophages inhibit aconitase in tumor cells. Inhibition involves the iron-sulfur prosthetic group and is reversible. *J. Clin. Invest.* **1986**, *78*, 790−797. (e) Drapier, J. C.; Pellat, C.; Henry, Y. Generation of EPR-detectable nitrosyl-iron complexes in tumor target cells cocultured with activated macrophages. *J. Biol. Chem.* **1991**, *266*, 10162−10167.

(18) Fitzpatrick, J.; Kim, E. Synthetic modeling chemistry of iron-sulfur clusters in nitric oxide signaling. *Acc. Chem. Res.* **2015**, *48*, 2453−2461.

(19) (a) Tran, C. T.; Kim, E. Acid-dependent degradation of a [2Fe-2S] cluster by nitric oxide. *Inorg. Chem.* **2012**, *51*, 10086−10088. (b) Tran, C. T.; Williard, P. G.; Kim, E. Nitric oxide reactivity of [2Fe-2S] clusters leading to H_2S generation. *J. Am. Chem. Soc.* **2014**, *136*, 11874−11877.

(20) Harrop, T. C.; Tonzetich, Z. J.; Reisner, E.; Lippard, S. J. Reactions of synthetic [2Fe-2S] and [4Fe-4S] clusters with nitric oxide and nitrosothiols. *J. Am. Chem. Soc.* **2008**, *130*, 15602−15610.

(21) Clarke, P. H. Hydrogen sulphide production by bacteria. *J. Gen. Microbiol.* **1953**, *8*, 397−407.

(22) Chen, B.; Li, W.; Lv, C.; Zhao, M.; Jin, H.; Jin, H.; Du, J.; Zhang, L.; Tang, X. Fluorescent probe for highly selective and sensitive detection of hydrogen sulfide in living cells and cardiac tissues. *Analyst* **2013**, *138*, 946−951.

(23) (a) Harrop, T. C.; Song, D.; Lippard, S. J. Reactivity pathways for nitric oxide and nitrosonium with iron complexes in biologically relevant sulfur coordination spheres. *J. Inorg. Biochem.* **2007**, *101*, 1730−1738. (b) Tsai, F. T.; Chiou, S. J.; Tsai, M. C.; Tsai, M. L.; Huang, H. W.; Chiang, M. H.; Liaw, W. F. Dinitrosyl iron complexes (DNICs) $[L_2Fe(NO)_2]^-$ (L = thiolate): interconversion among $\{Fe(NO)_2\}^9$ DNICs, $\{Fe(NO)_2\}^{10}$ DNICs, and [2Fe-2S] clusters, and the critical role of the thiolate ligands in regulating NO release of DNICs. *Inorg. Chem.* **2005**, *44*, 5872−5881.

(24) (a) Strasdeit, H.; Krebs, B.; Henkel, G. Synthesis and Structure of $[Fe(SPh)_2(NO)_2]^-$, the "Monomer" of Roussin's Phenyl Ester. *Z. Naturforsch., B: J. Chem. Sci.* **1986**, *41*, 1357−1362. (b) Tsai, M. C.; Tsai, F. T.; Lu, T. T.; Tsai, M. L.; Wei, Y. C.; Hsu, I. J.; Lee, J. F.; Liaw, W. F. Relative Binding Affinity of Thiolate, Imidazolate, Phenoxide, and Nitrite Toward the $\{Fe(NO)_2\}$ Motif of Dinitrosyl Iron Complexes (DNICs): The Characteristic Pre-Edge Energy of $\{Fe(NO)_2\}^9$ DNICs. *Inorg. Chem.* **2009**, *48*, 9579−9591.

(25) The formation of disulfide from the two-step conversion of **1** to **2** was also observed. Both steps generate disulfide. However, the exact quantification was hampered by the difficulties in isolating the intermediate.

(26) Roussin, M. L. Recherches sur les nitrosulfures doubles de fer (nouvelle classe de sels). *Ann. Chim. Phys.* **1858**, *52*, 285−303.

(27) Chmura, A.; Szacilowski, K.; Waksmundzka-Gora, A.; Stasicka, Z. Photochemistry of the $[Fe_4((_3\text{-}S)_3(NO)_7]^-$ complex in the presence of S-nucleophiles: a spectroscopic study. *Nitric Oxide* **2006**, *14* (3), 247−260.

(28) Meister, A. Glutathione metabolism and its selective modification. *J. Biol. Chem.* **1988**, *263*, 17205−17208.

(29) Hamilton-Brehm, S. D.; Schut, G. J.; Adams, M. W. Antimicrobial activity of the iron-sulfur nitroso compound Roussin's black salt $[Fe_4S_3(NO)_7]$ on the hyperthermophilic archaeon Pyrococcus furiosus. *Appl. Environ. Microbiol.* **2009**, *75*, 1820−1825.

(30) (a) Wang, R. Physiological implications of hydrogen sulfide: a whiff exploration that blossomed. *Physiol. Rev.* **2012**, *92*, 791−896. (b) Li, L.; Rose, P.; Moore, P. K. Hydrogen sulfide and cell signaling. *Annu. Rev. Pharmacol. Toxicol.* **2011**, *51*, 169−187.

(31) (a) Lo, F. C.; Lee, J. F.; Liaw, W. F.; Hsu, I. J.; Tsai, Y. F.; Chan, S. I.; Yu, S. S. The metal core structures in the recombinant Escherichia coli transcriptional factor SoxR. *Chem. - Eur. J.* **2012**, *18*, 2565−2577. (b) Rogers, P. A.; Ding, H. L-cysteine-mediated destabilization of dinitrosyl iron complexes in proteins. *J. Biol. Chem.* **2001**, *276*, 30980−30986. (c) Grabarczyk, D. B.; Ash, P. A.; Vincent, K. A. Infrared spectroscopy provides insight into the role of dioxygen in the nitrosylation pathway of a [2Fe2S] cluster iron-sulfur protein. *J. Am. Chem. Soc.* **2014**, *136*, 11236−11239. (d) Tinberg, C. E.; Tonzetich, Z. J.; Wang, H.; Do, L. H.; Yoda, Y.; Cramer, S. P.; Lippard, S. J. Characterization of iron dinitrosyl species formed in the reaction of nitric oxide with a biological Rieske center. *J. Am. Chem. Soc.* **2010**, *132*, 18168−18176.

(32) Cheng, Z.; Landry, A. P.; Wang, Y.; Ding, H. Binding of Nitric Oxide in CDGSH-type [2Fe-2S] Clusters of the Human Mitochondrial Protein Miner2. *J. Biol. Chem.* **2017**, *292*, 3146−3153.

(33) Tonzetich, Z. J.; Wang, H.; Mitra, D.; Tinberg, C. E.; Do, L. H.; Jenney, F. E., Jr.; Adams, M. W.; Cramer, S. P.; Lippard, S. J. Identification of protein-bound dinitrosyl iron complexes by nuclear resonance vibrational spectroscopy. *J. Am. Chem. Soc.* **2010**, *132*, 6914−6916.

(34) Ekanger, L. A.; Oyala, P. H.; Moradian, A.; Sweredoski, M. J.; Barton, J. K. Nitric Oxide Modulates Endonuclease III Redox Activity by a 800 mV Negative Shift upon [Fe4S4] Cluster Nitrosylation. *J. Am. Chem. Soc.* **2018**, *140*, 11800−11810.

(35) Serrano, P. N.; Wang, H.; Crack, J. C.; Prior, C.; Hutchings, M. I.; Thomson, A. J.; Kamali, S.; Yoda, Y.; Zhao, J.; Hu, M. Y.; Alp, E. E.; Oganesyan, V. S.; Le Brun, N. E.; Cramer, S. P. Nitrosylation of Nitric-Oxide-Sensing Regulatory Proteins Containing [4Fe-4S] Clusters Gives Rise to Multiple Iron-Nitrosyl Complexes. *Angew. Chem., Int. Ed.* **2016**, *55*, 14575−14579.

(36) Grabarczyk, D. B.; Ash, P. A.; Myers, W. K.; Dodd, E. L.; Vincent, K. A. Dioxygen controls the nitrosylation reactions of a protein-bound [4Fe4S] cluster. *Dalton Trans.* **2019**, *48*, 13960−13970.

(37) Hagen, K. S.; Reynolds, J. G.; Holm, R. H. Definition of Reaction Sequences Resulting in Self-Assembly of $[Fe_4S_4(SR)_4]^{2-}$ Clusters from Simple Reactants. *J. Am. Chem. Soc.* **1981**, *103*, 4054−4063.

https://doi.org/10.1021/acs.inorgchem.1c01328
Inorg. Chem. XXXX, XXX, XXX−XXX